A Global-Seasonal Assessment of Homogeneous Ice Nucleation in Cirrus Clouds and Relative Estimates of Cloud Radiative Effect

David L. Mitchell[1] and Anne Garnier[2]

1. Desert Research Institute, Reno, Nevada, USA
2. Analytical Mechanics Associates, Hampton, Virginia, USA

Het cirrus

Hom cirrus

CLIMATE PROGRAM OFFICE

ADVANCING SCIENTIFIC UNDERSTANDING OF CLIMATE, IMPROVING SOCIETY'S ABILITY TO PLAN AND RESPOND

Desert Research Institute

CESM Atmosphere Model Working Group Meeting, 12 – 14 Feb. 2024

Improvements to the CALIPSO cirrus cloud retrieval of Mitchell et al. (2018, ACP)

1. **Ice particle number concentration** no longer depends on estimates of IWC but rather depends on optical probe measurements of ice particle size distribution (PSD) number concentration and projected area:

$$N = \left(\frac{N}{A_{PSD}} \right)_{\beta_{eff}} \times \frac{\left(1/Q_{abs,eff}(12\mu m)\right)_{\beta_{eff}} \times \tau_{abs}(12.05\mu m)}{\Delta z_{eq}} \quad \textbf{(1)}$$

2. **Estimation of in situ IWC has been improved**, with better estimates of small ice particle mass (Erfani & Mitchell, 2016, ACP) yielding better agreement between β_{eff} calculated from in situ PSD measurements and IIR β_{eff}.

3. **Improved retrieval equation for effective diameter** based on theory and two strong empirical relationships:

$$D_e = \frac{3}{2} \times \frac{IWC}{\rho_i \cdot A_{PSD}} = \frac{3}{2 \cdot \rho_i} \times \left(\frac{N}{A_{PSD}} \right)_{\beta_{eff}} \times \left(\frac{IWC}{N} \right)_{\beta_{eff}} \quad \textbf{(2)}$$

Theory, Mitchell, JAS, 2002

From which we derive $IWC = \frac{\rho_i}{3} \times \alpha_{ext} \times D_e$ with $\alpha_{ext} = \frac{2.\left(1/Q_{abs,eff}(12\mu m)\right)_{\beta_{eff}}}{\Delta z_{eq}} \times \tau_{abs}(12.05\mu m)$ **(3)**

KEY POINTS:

1. Only single-layer ice clouds are sampled that are semi-transparent to the CALIOP lidar.

2. Most of the clouds sampled have a visible optical depth $\tau < 3$.

3. Retrieved cloud properties from CALIPSO Infrared Imaging Radiometer (IIR) correspond to cloud layers and not in-cloud profiles. Larger uncertainties at small optical depth.

4. Sampled clouds have a radiative temperature ≤ 235 K (-38 °C).

5. The N/A_{PSD}-β_{eff}, N/IWC-β_{eff}, and $1/ Q_{abs,eff}$ (12 µm)- β_{eff} relationships were developed from cirrus cloud PSD measurements from several field campaigns using the same methodology as in Mitchell et al. (2018, ACP).

6. The following analysis is based on 4 years of CALIPSO data.

Comparison with global cirrus cloud climatology of Krämer et al. (2020, ACP) based on aircraft measurements (black curves). Reasonable agreement for all IIR samples (~ 0.005 < τ < ~ 3; τ = cloud optical depth) => blue curves. Less agreement for orange & red curves where 0.3 < τ < 3 and uncertainty is lowest. Orange & light-blue curves are for tropics only. Bars & shading give percentiles (10%, 25%, 75% & 90%).

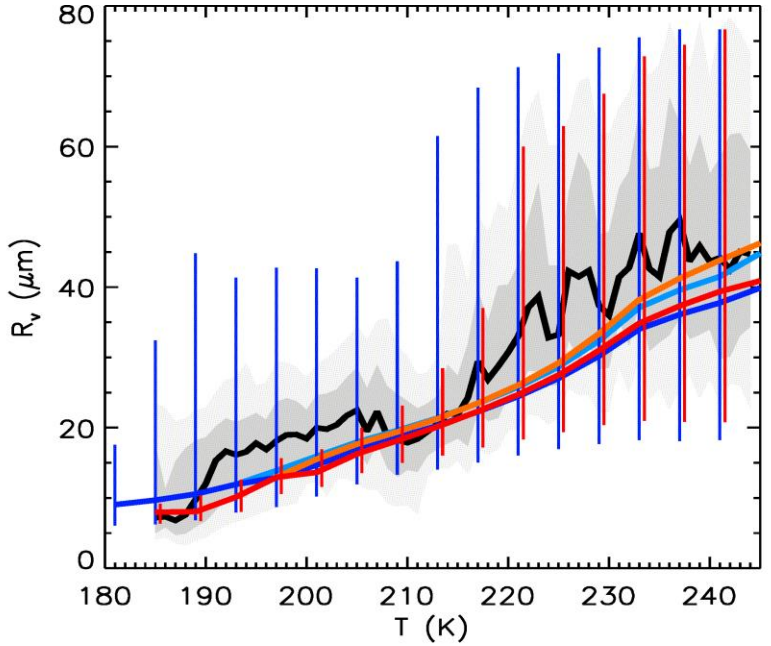

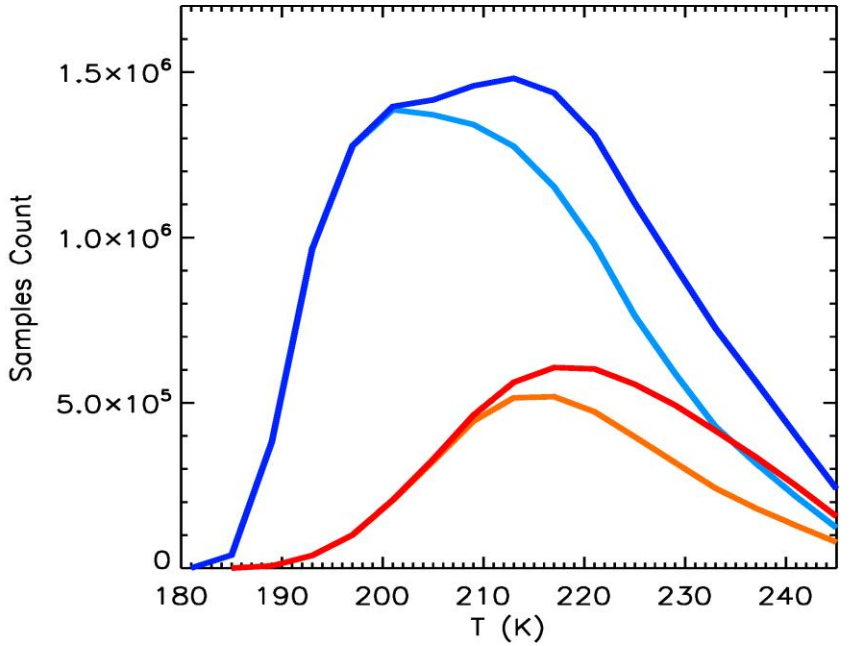

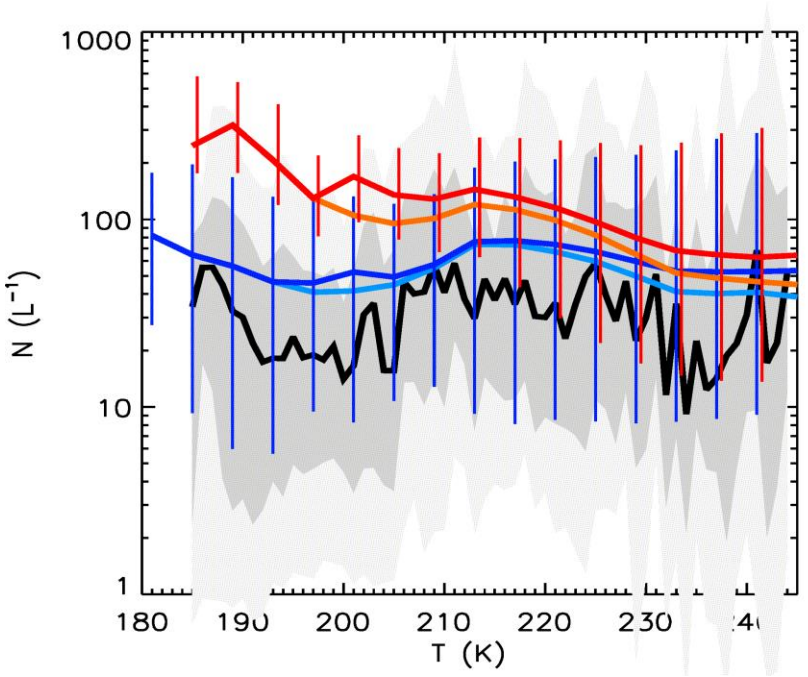

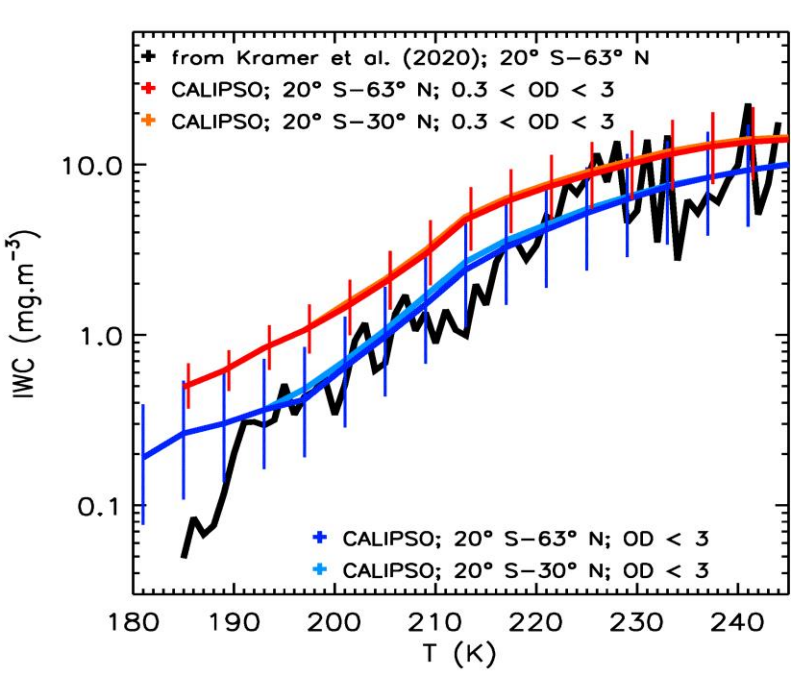

Some research findings not shown (due to time constraints):

1. **When homogeneous ice nucleation (i.e., hom) is relatively active (based on higher N), N and IWC are most affected with relatively high values. When hom is most active (as observed over land), D_e decreases.**

2. **Therefore, to distinguish between two types of cirrus clouds, where one is formed through heterogeneous ice nucleation (i.e., het) while hom is also active in the other type, relate cirrus cloud properties to the cloud visible extinction coefficient:**

$$\alpha_{ext} = \frac{3\ IWC}{\rho_i\ D_e}$$

where ρ_i is the bulk density of ice.

Based on all samples over oceans where ~ 0.005 < τ < ~ 3.
Color inside the triangles (from model) uses the same color legend.

IWC in T_r vs. log(α_{ext}) space

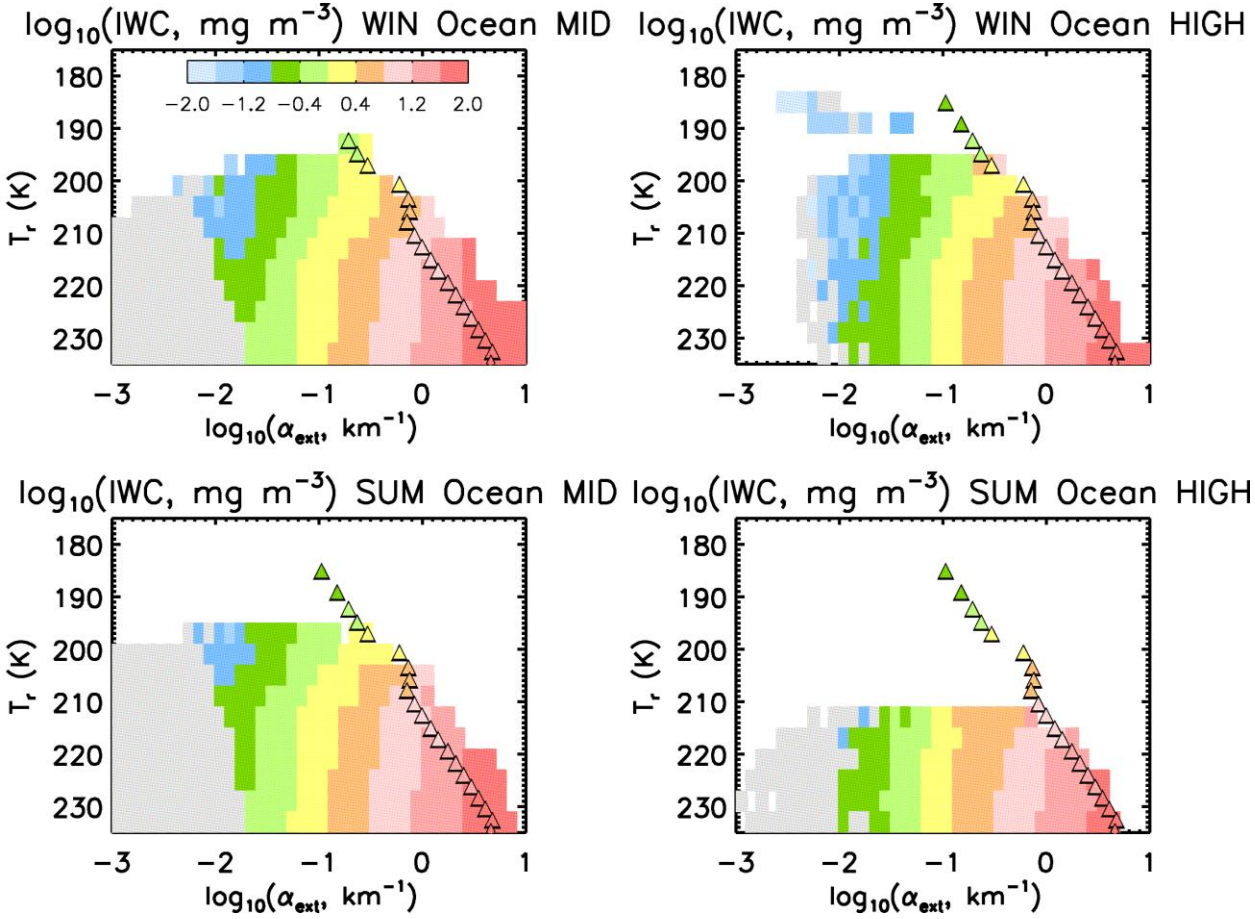

N_i in T_r vs. log(α_{ext}) space

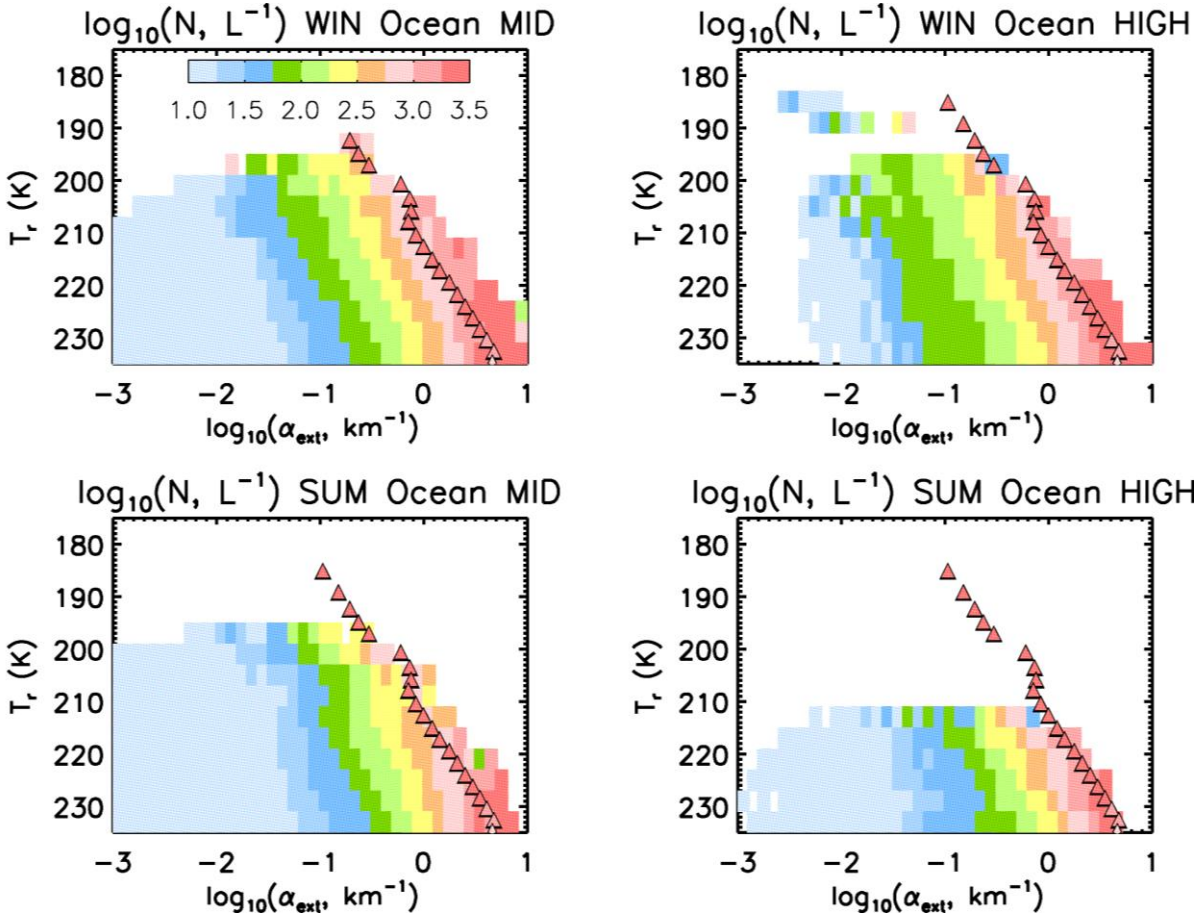

SIMPLE MODEL USED TO PREDICT HOM MICROPHYSICAL CONDITIONS

Clausius-Clapeyron Equation:

$e_{si} = e_{s0} \exp\left[\frac{L_s}{R_g}\left(\frac{1}{T_0} - \frac{1}{T}\right)\right]$ e_{si} = water vapor pressure at ice saturation, L_s = latent heat of sublimation, R_g = gas constant

Supersaturation required for homogeneous ice nucleation:

$e_s / e_{si} = \exp\left[\frac{L_f}{R_g}\left(\frac{1}{T} - \frac{1}{T_0}\right)\right]$ e_s = water vapor pressure at water saturation, L_f = latent heat of fusion

$S_i^f = 1.0 + 0.305\ (e_s/e_{si})$ S_i^f = supersaturation where homogeneous ice nucleation occurs

$e_{hom} = S_i^f\ e_{si}$ e_{hom} = water vapor pressure at S_i^f

Vapor densities are obtained from the gas law.
Maximum IWC resulting from homogeneous ice nucleation (hom):

$$\mathbf{IWC_{hom} = \rho_{hom} - \rho_{si}}$$

IWC_{hom} is plotted with triangles against T_r in previous plot, with values given by the color legend.
D_e and N were predicted from IWC_{hom}, empirical D_{mean}-T relationships from the tropics (CEPEX) and midlatitudes (SPARTICUS), ice particle mass- and area-size expressions in Erfani & Mitchell (2016, ACP) and Eq. 7 in Mitchell et al. (2020, ACP) that converts D_e to D_{mean} for exponential PSDs. **Thus, the triangles plotted for IWC, D_e, and N correspond to pure hom conditions.**

Based on all samples over oceans where ~ 0.005 < τ < ~ 3.
Color inside the triangles (from model) uses the same color legend.

D_e in T_r vs. log(α_{ext}) space

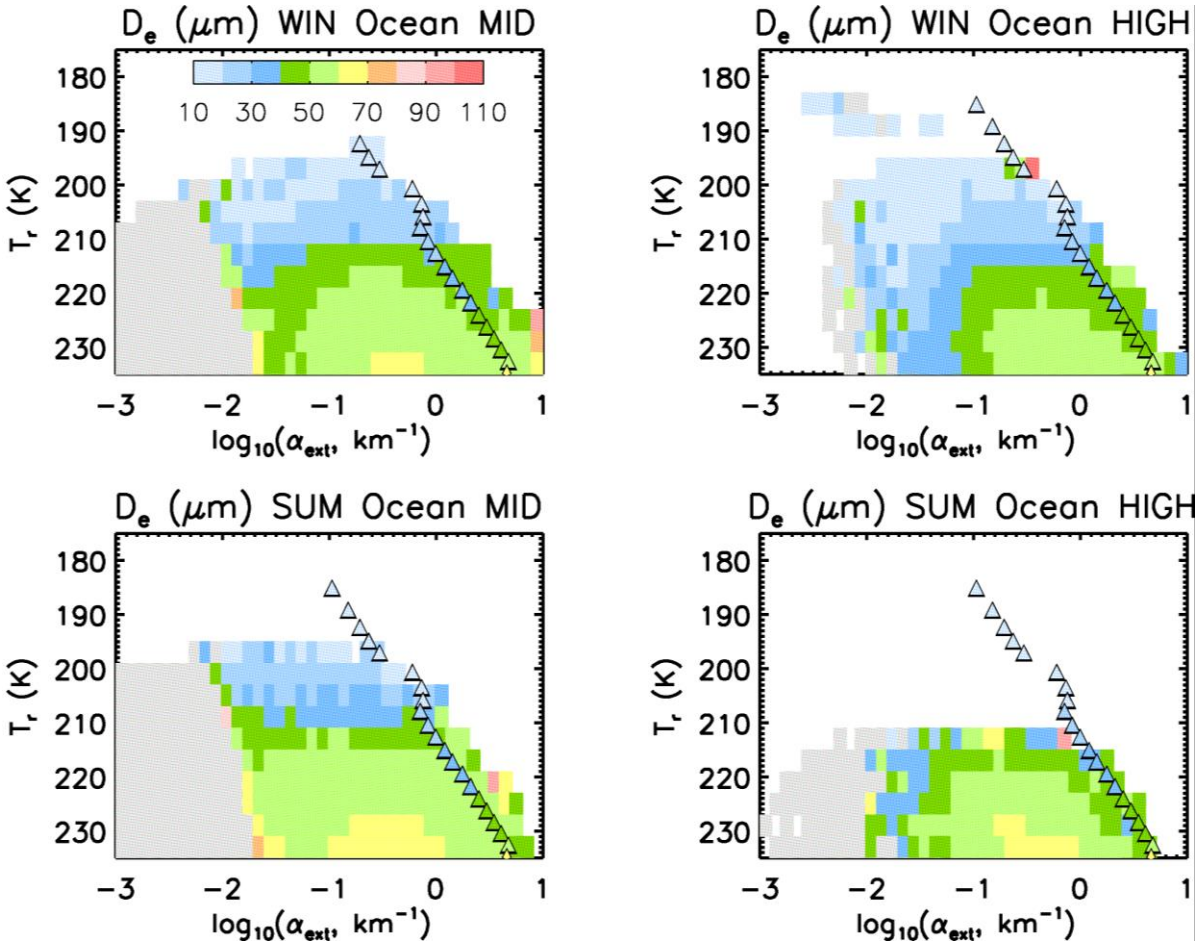

log(counts) in T_r vs. log(α_{ext}) space

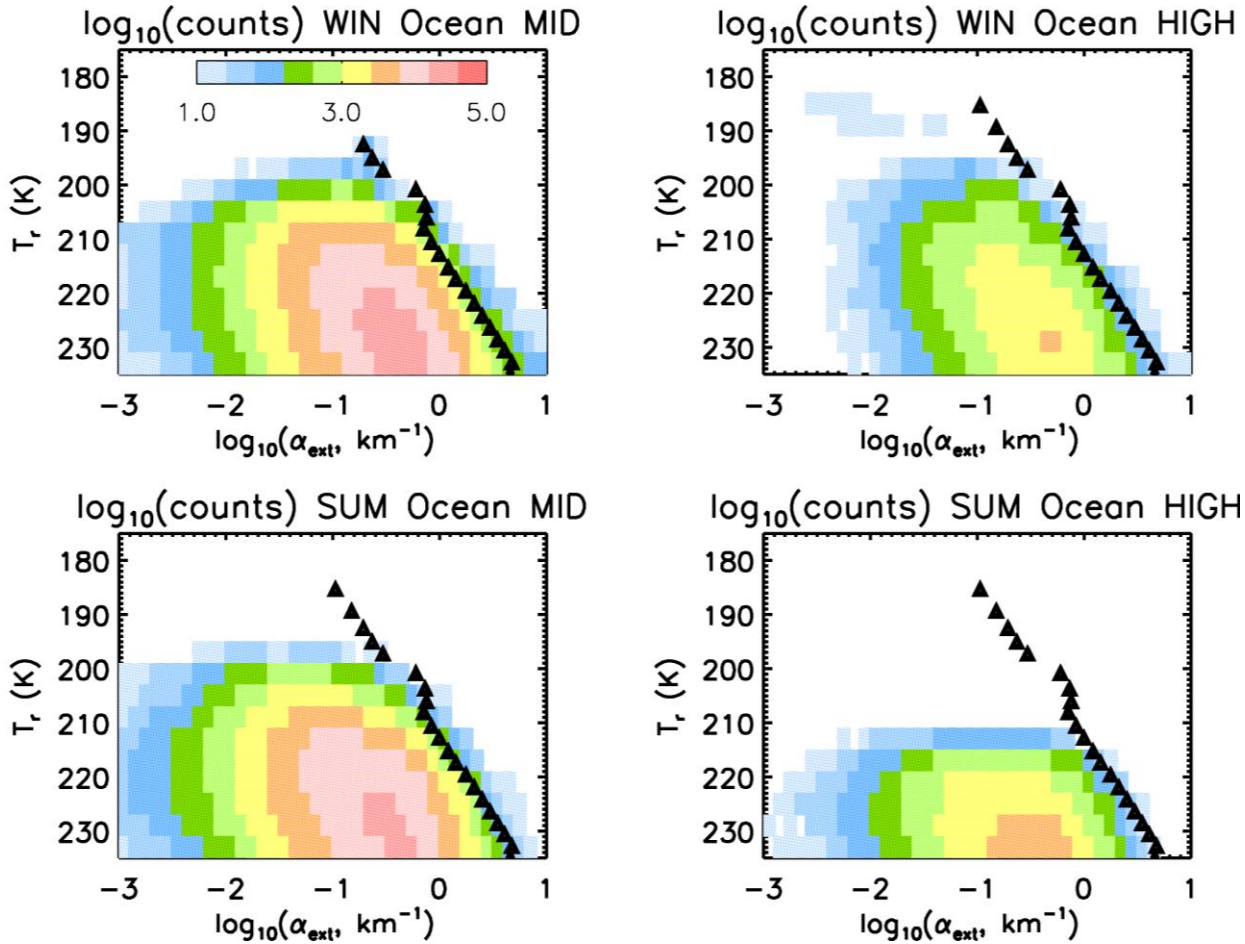

Estimating the fraction of cirrus strongly impacted by hom

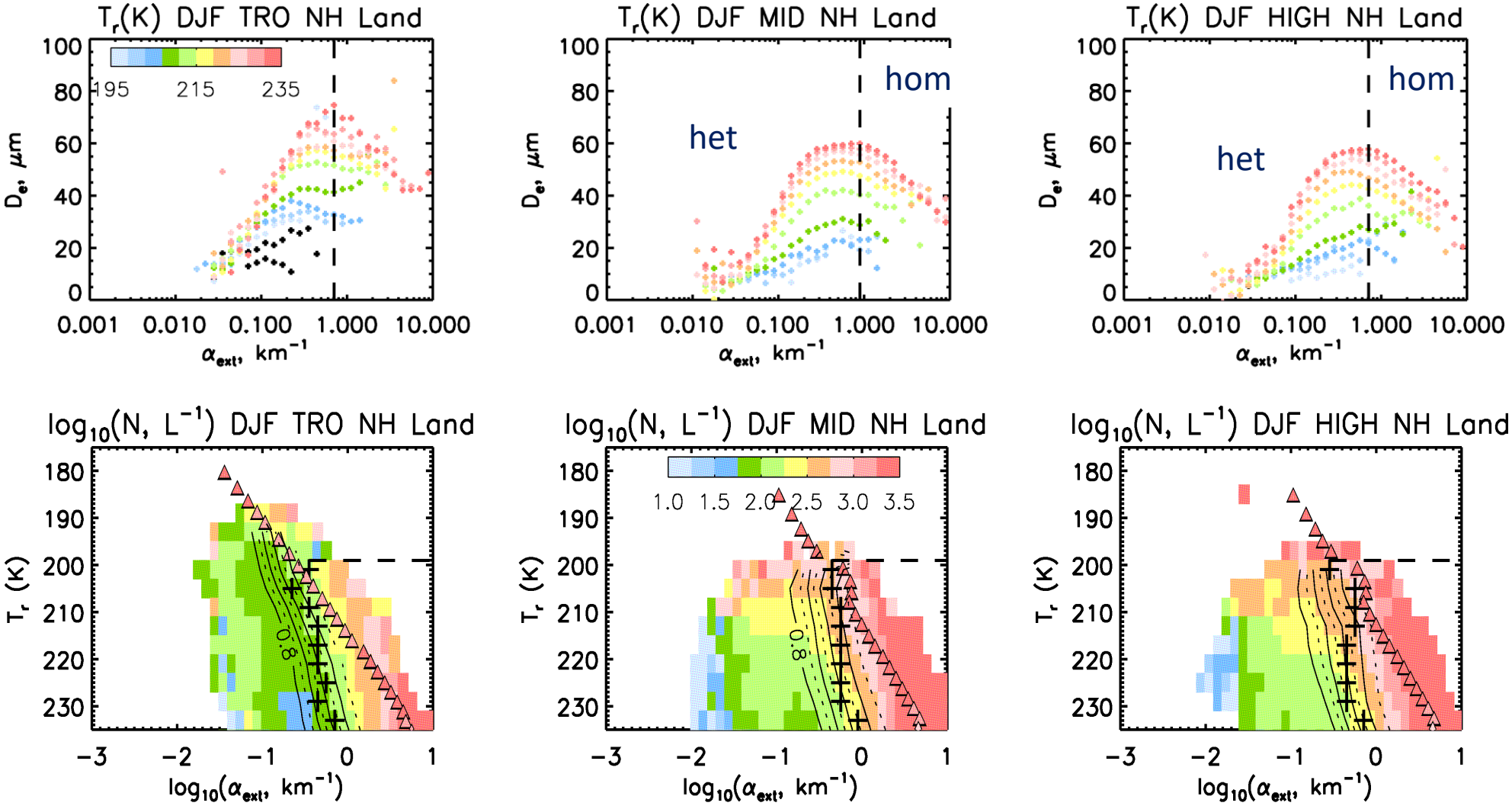

When D_e is related to α_{ext} at 4 K intervals (colors), the peak D_e value marks the het-hom transition where higher N from hom results in lower D_e due to vapor competition effects. Dashed line is example for 231-235 K.

At lower T_r, evidence of hom (i.e., the D_e maximum) vanishes, indicated by the horizontal dashed line. The black "+" signs indicate D_e maximums. **The enclosed region is strongly affected by hom.**

Solid & dashed curves show the fraction of all samples (on right side for a given T_r) in 10% increments.

Liquid Origin hom In Situ hom Liquid Origin het In Situ het

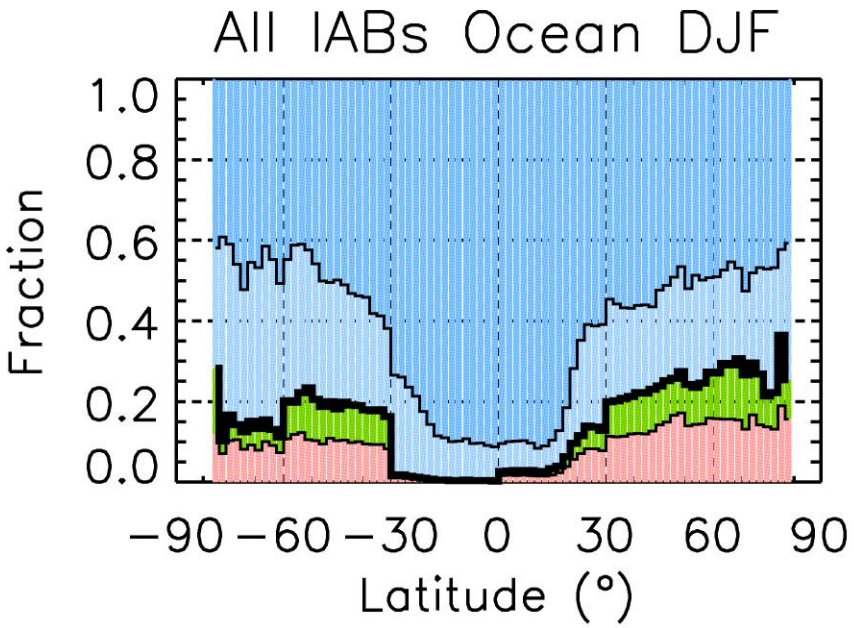

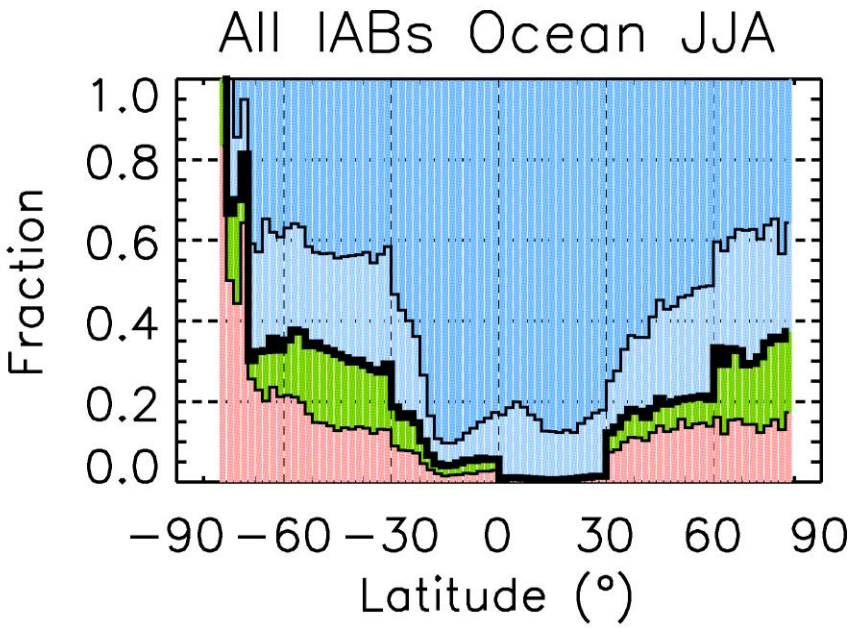

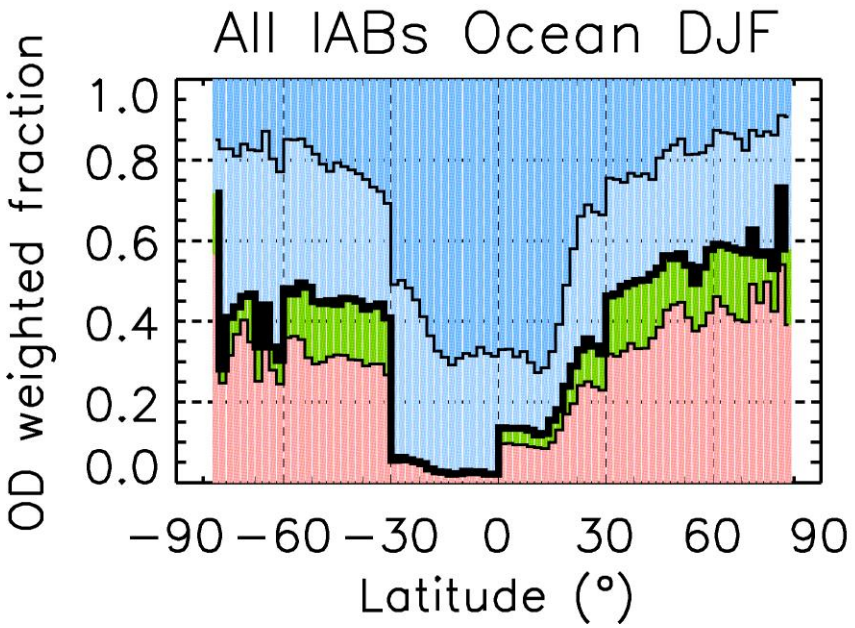

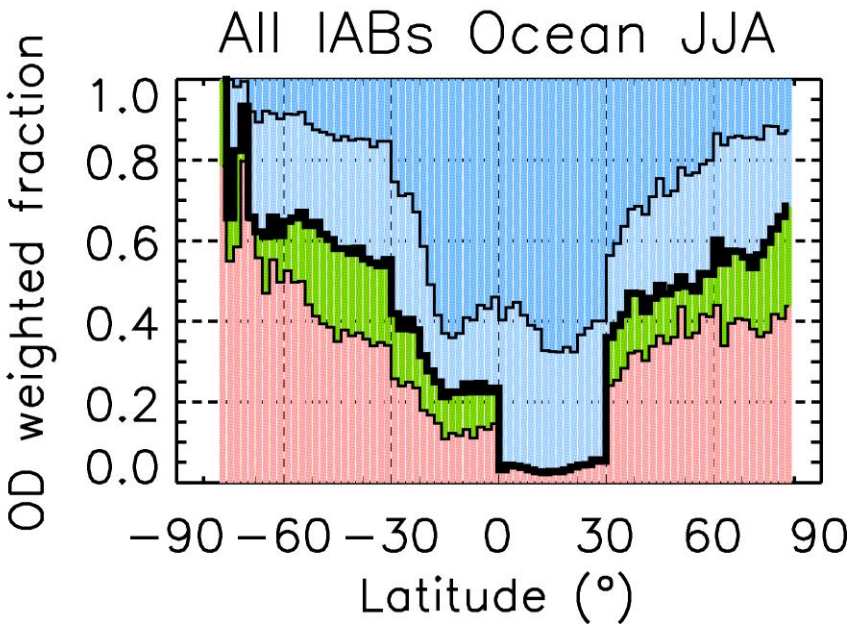

Zonal means of the hom fraction are shown by the thick black histogram while blue colors indicate het cirrus (light blue for liquid origin, darker blue for in situ cirrus). Pink indicates the hom fraction for liquid origin cirrus while green is for in situ cirrus clouds. The bottom panels show the product of hom fraction x optical depth as a measure of the cloud radiative effect. **During winter outside the tropics, this τ-weighted hom fraction tends to be > 50%, indicating hom-affected cirrus clouds contribute substantially to the earth's radiation budget.**

Seasonal changes in dust conc. inversely proportional to hom fraction

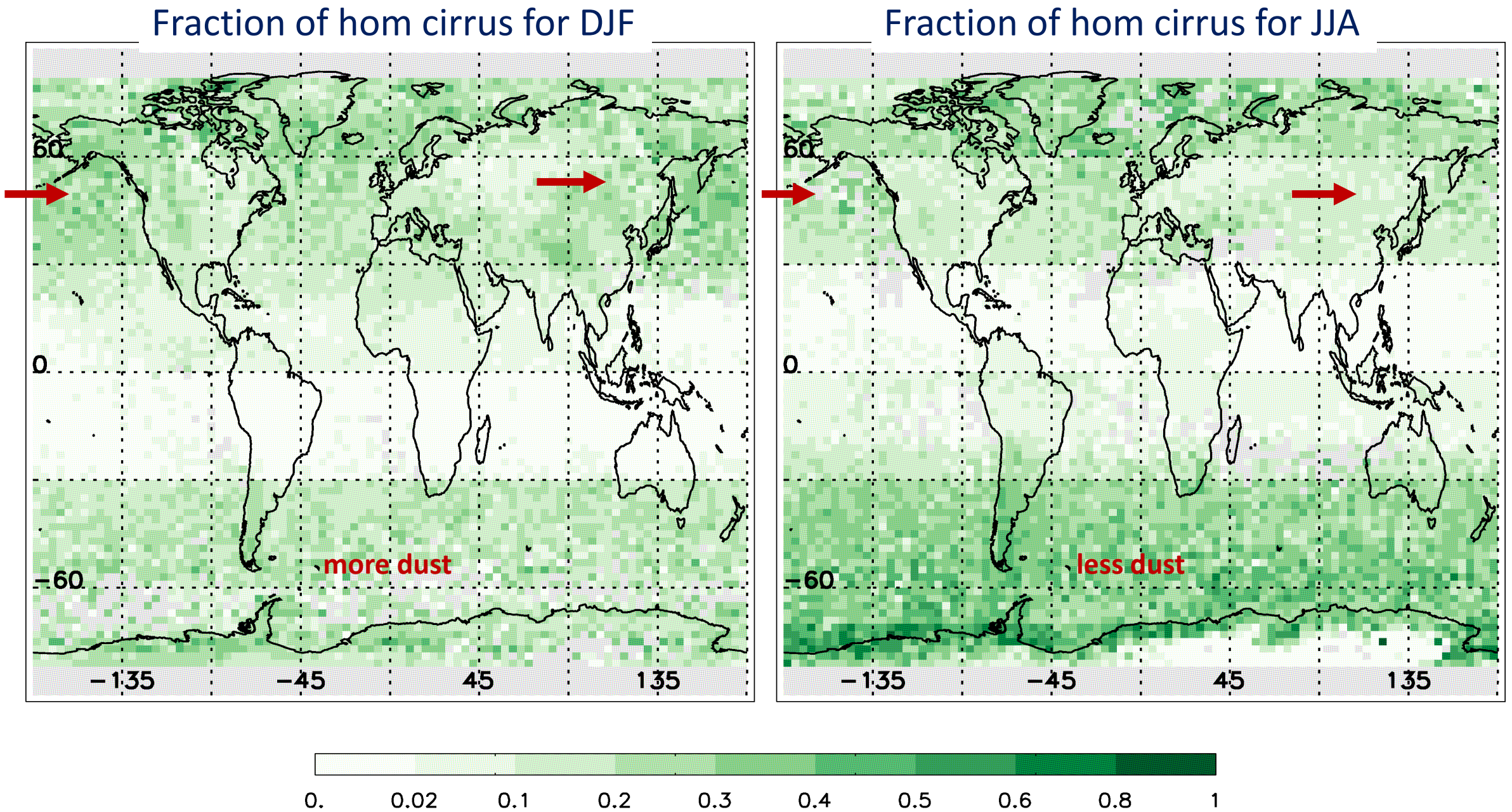

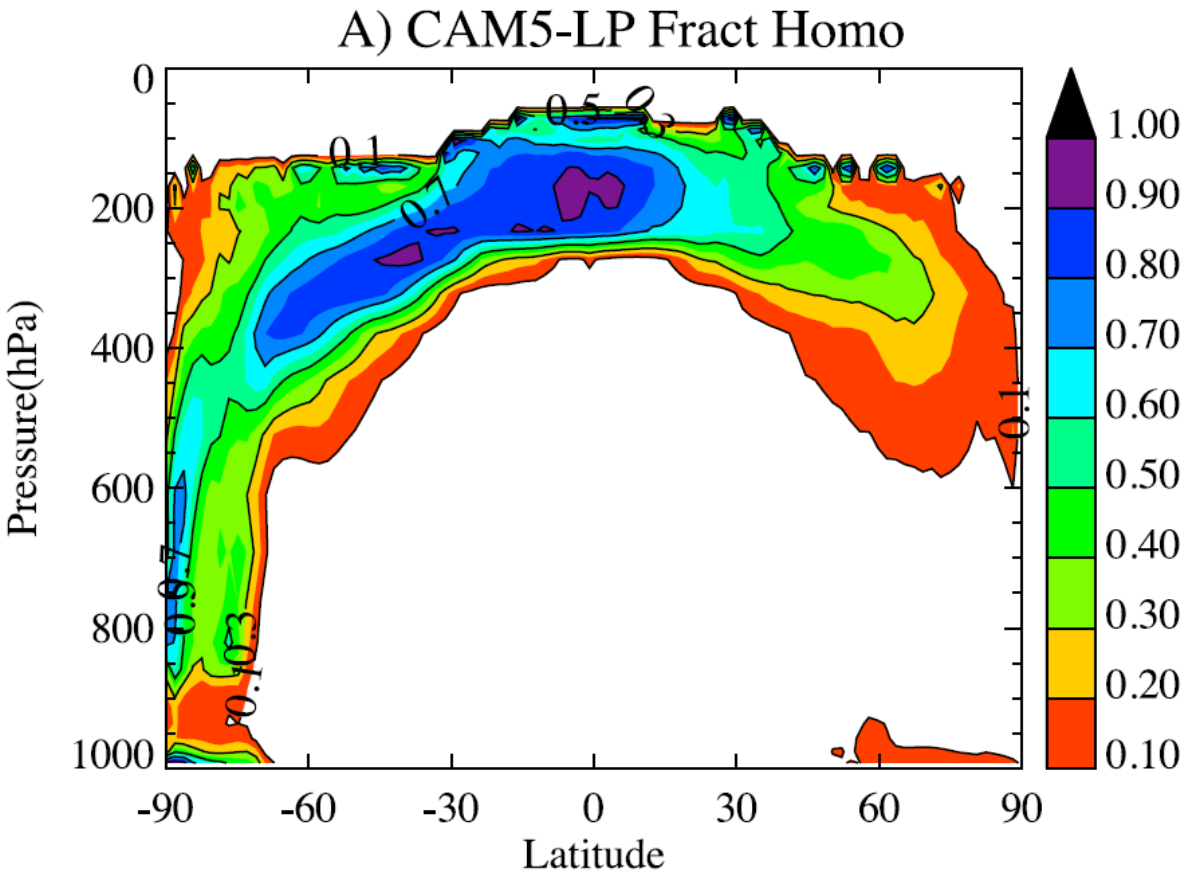

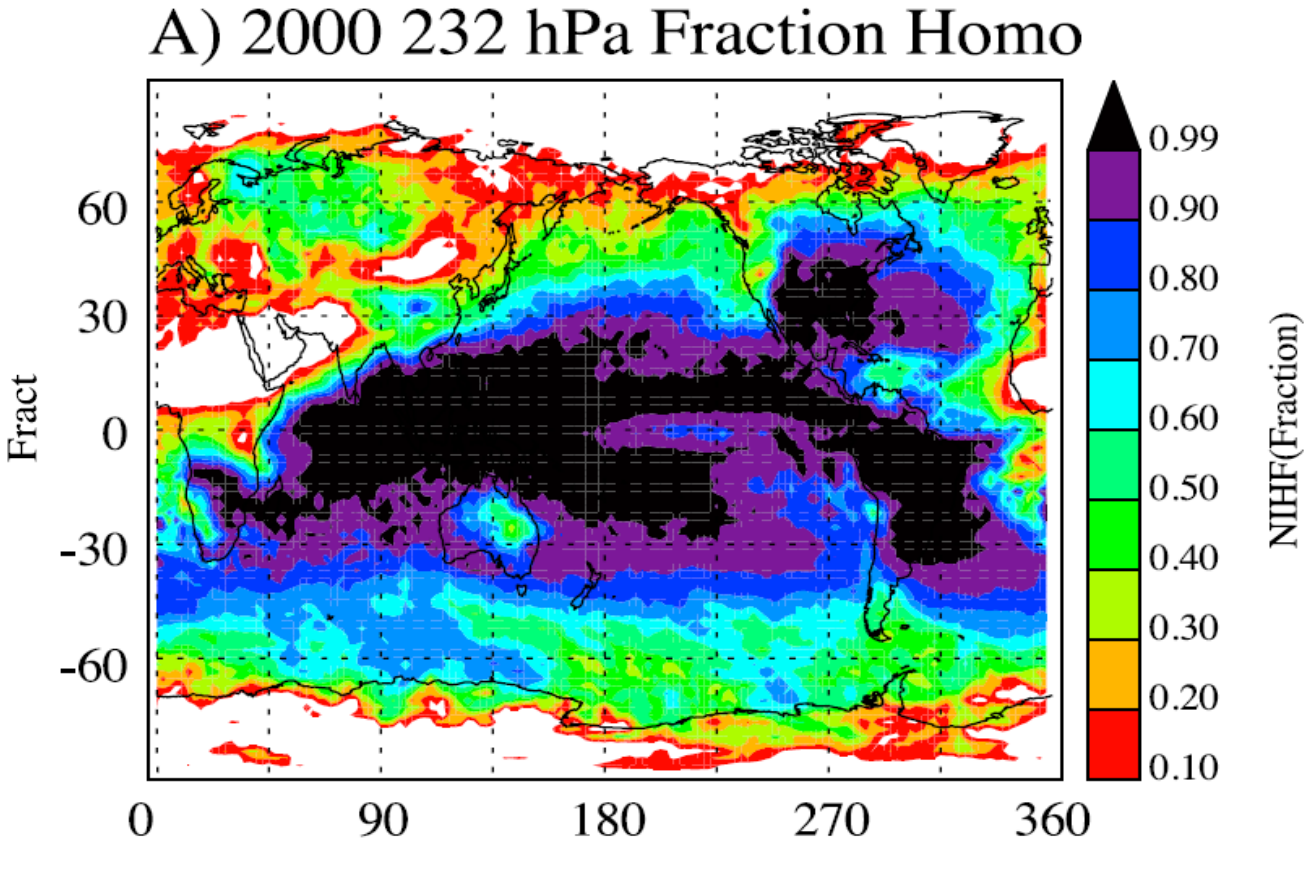

From Gettelman, A., X. Liu, D. Barahona, U. Lohmann, and C. Chen (2012), Climate impacts of ice nucleation, J. Geophys. Res., 117, D20201, doi:10.1029/2012JD017950.

Left panel: Zonal mean fraction of ice crystals produced through hom in the year 2000 based on standard version of CAM5.

Right panel: Map of 232 hPa fraction of ice crystals nucleated due to homogeneous freezing in the standard version of CAM5 for the year 2000 (corresponds to the same field as in the left panel).

CALIPSO estimate of hom fraction is limited to $\tau < 3$, thus missing deep convection in tropics and elsewhere (esp. in summer).

SUMMARY

1. A new CALIPSO retrieval for cirrus clouds was developed and used to investigate hom.
2. Agreement found between hom theory and CALIPSO retrievals that corresponded to the region of “pure hom”.
3. Retrievals of SW extinction, D_e, and cloud temperature were used to estimate the fraction of cirrus clouds strongly affected by hom.
4. Over ocean outside the tropics in winter, the zonal mean fraction of hom-affected cirrus generally ranges between 20% and 35%, with comparable contributions from in situ and liquid origin cirrus.
5. The τ-weighted fraction for hom-affected cirrus was used as a relative proxy for the cloud radiative effect (CRE). Over oceans outside the tropics during winter, this τ-weighted fraction was > 50%, showing that hom-cirrus are radiatively important.
6. The hom fraction appears anticorrelated with inferred mineral dust concentration; more research is needed here.

OTHER SLIDES

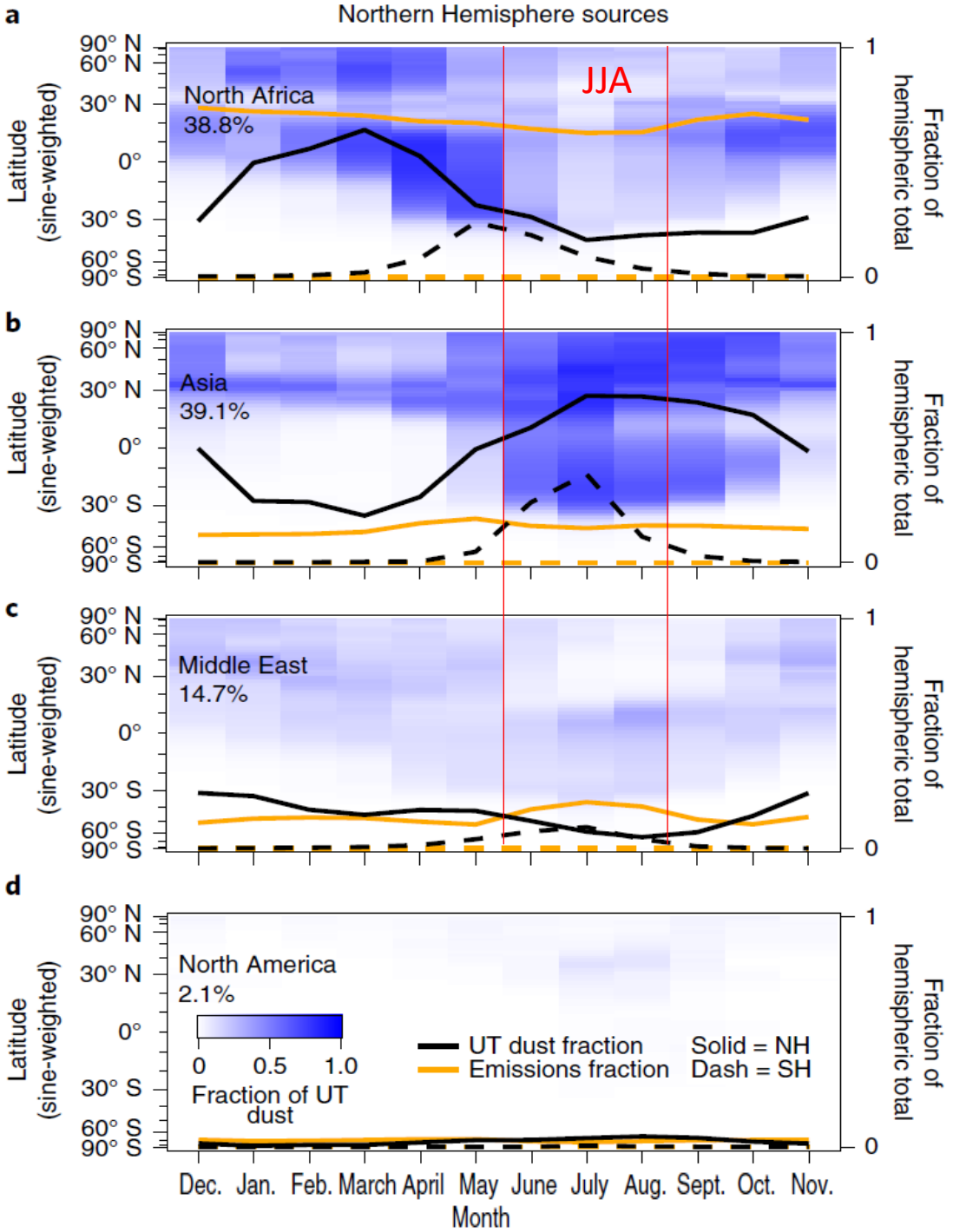

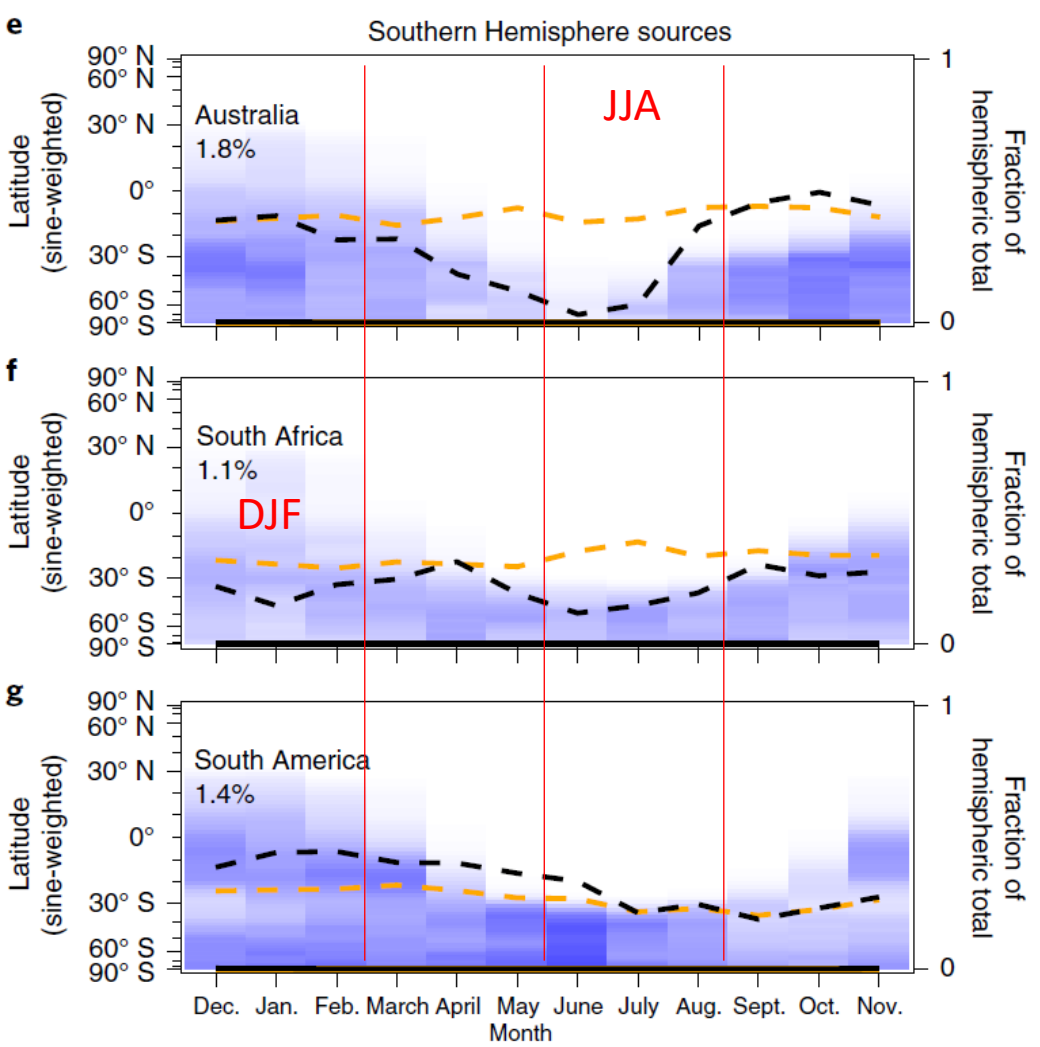

Note: The blue histograms show the total UT dust fraction for a given latitude, and NH sources do not contribute at lats. > ~ 40 S. Over the Southern Ocean, only SH sources contribute, with mostly South America (SA) contributing during JJA (winter). This suggests lower dust levels during JJA if SA dust emissions do not increase then.

Figure 3 from Froyd et al., Nature Geoscience, 2022. Annual cycle of UT dust sourced from each desert emission zone from the revised CESM/CARMA model. a–g, Shading indicates each source's fractional contribution to UT dust mass as a function of latitude (left axis) and season. Annual averages are listed as percentages. Lines (right axis) compare fractional UT concentrations (black) and surface emissions (orange) within the Northern (solid; NH) and Southern (dash; SH) Hemispheres.

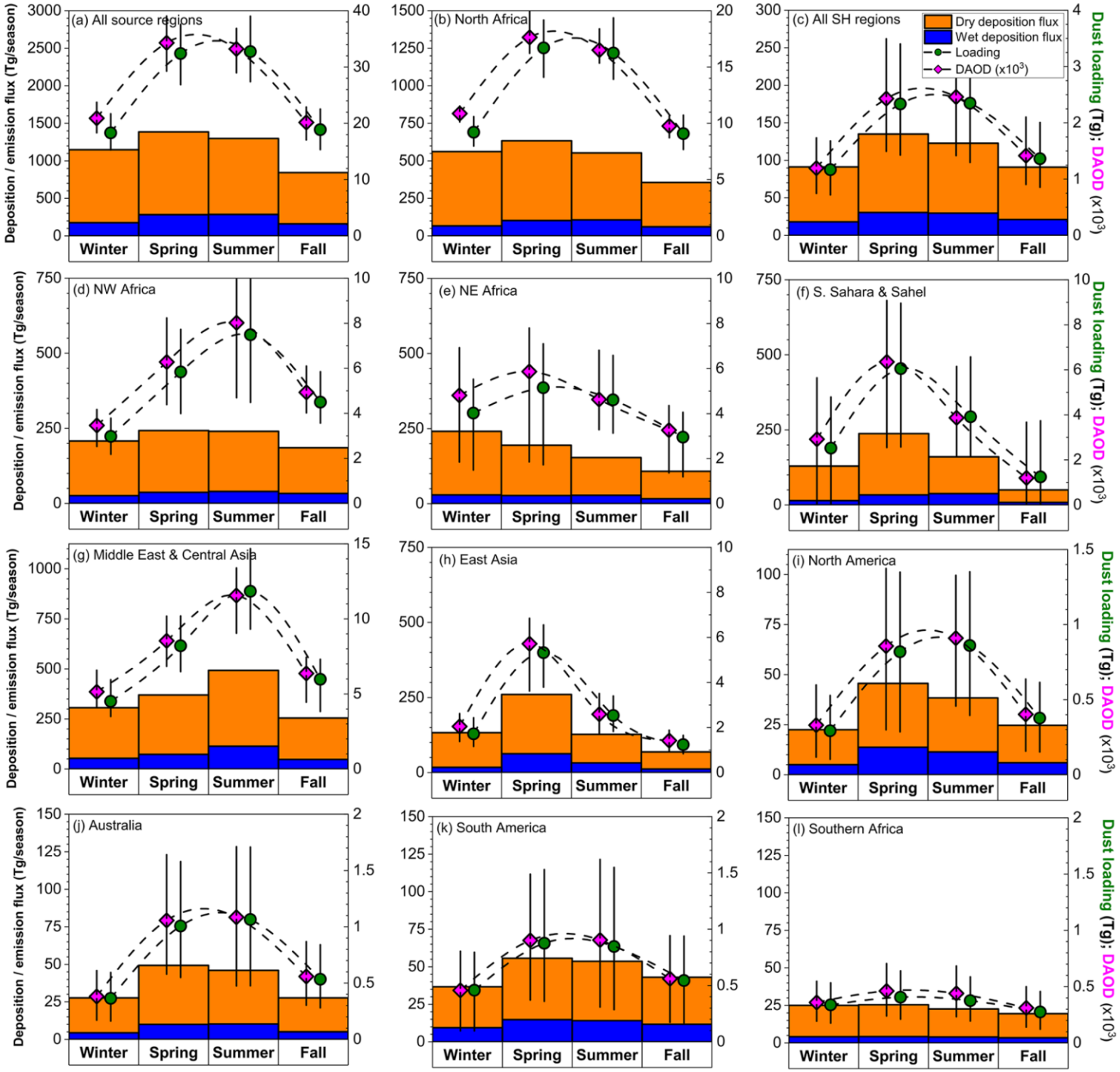

Figure 4 from *Kok et al., 2021: Contribution of the world's main dust source regions to the global cycle of desert dust, ACP, 21, 8169–8193*, https://doi.org/10.5194/acp-21-8169-2021.

Seasonal contributions of each source region to the global dust cycle. Shown are the seasonal cycles of the wet deposition flux (blue bars and left axis), dry deposition flux (orange bars and left axis), dust loading (green circles and right axis), and dust aerosol optical depth or DAOD (magenta diamonds and right axis) generated by (a) all source regions, (b) all North African source regions, (c) all Southern Hemisphere source regions, and (d–l) each of the nine individual source regions. The sum of the seasonal wet and dry deposition fluxes is approximately equal (within a few percent) to the seasonal dust emission flux generated by each source region. Results for loading and DAOD are slightly offset horizontally for clarity. *Seasons refer to boreal seasons for global results (a) and to local seasons for all other panels*. Note that the vertical axis scale differs between source regions. Error bars denote 1 standard error from the median; error bars on deposition fluxes usually exceeded 100% and are not included for clarity.

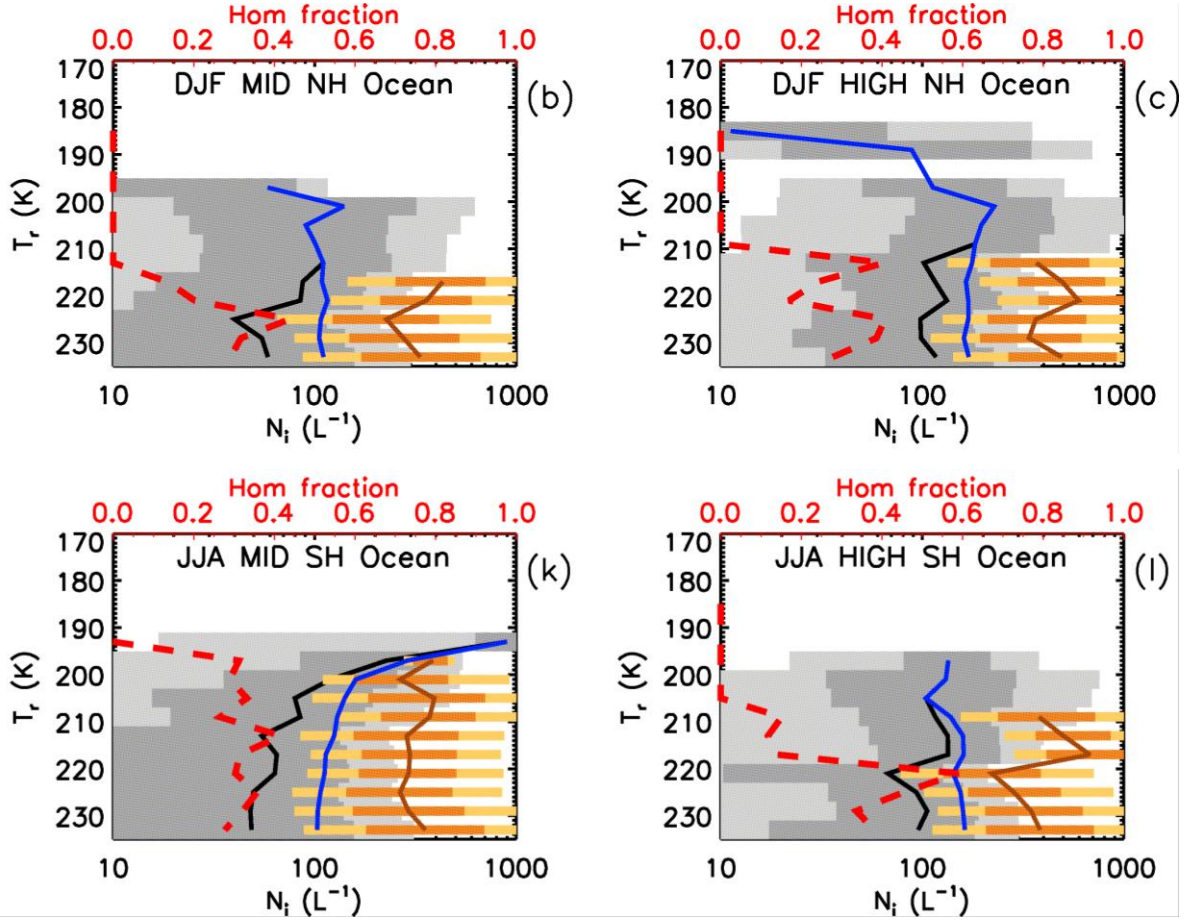

Temperature dependence of the hom fraction (red dashed) over oceans (~ 0.005 < τ < ~ 3) for the midlatitudes (MID) and high latitudes (HIGH) during winter in the northern (NH) and southern (SH) hemispheres. Also shown are median N_i profiles for all cirrus (blue), for het cirrus (black), and for hom cirrus (orange). The 25 to 75 percentile range is indicated by darker grey and orange shading for het cirrus and hom cirrus, with lighter shading for the 10 to 90 percentile range.

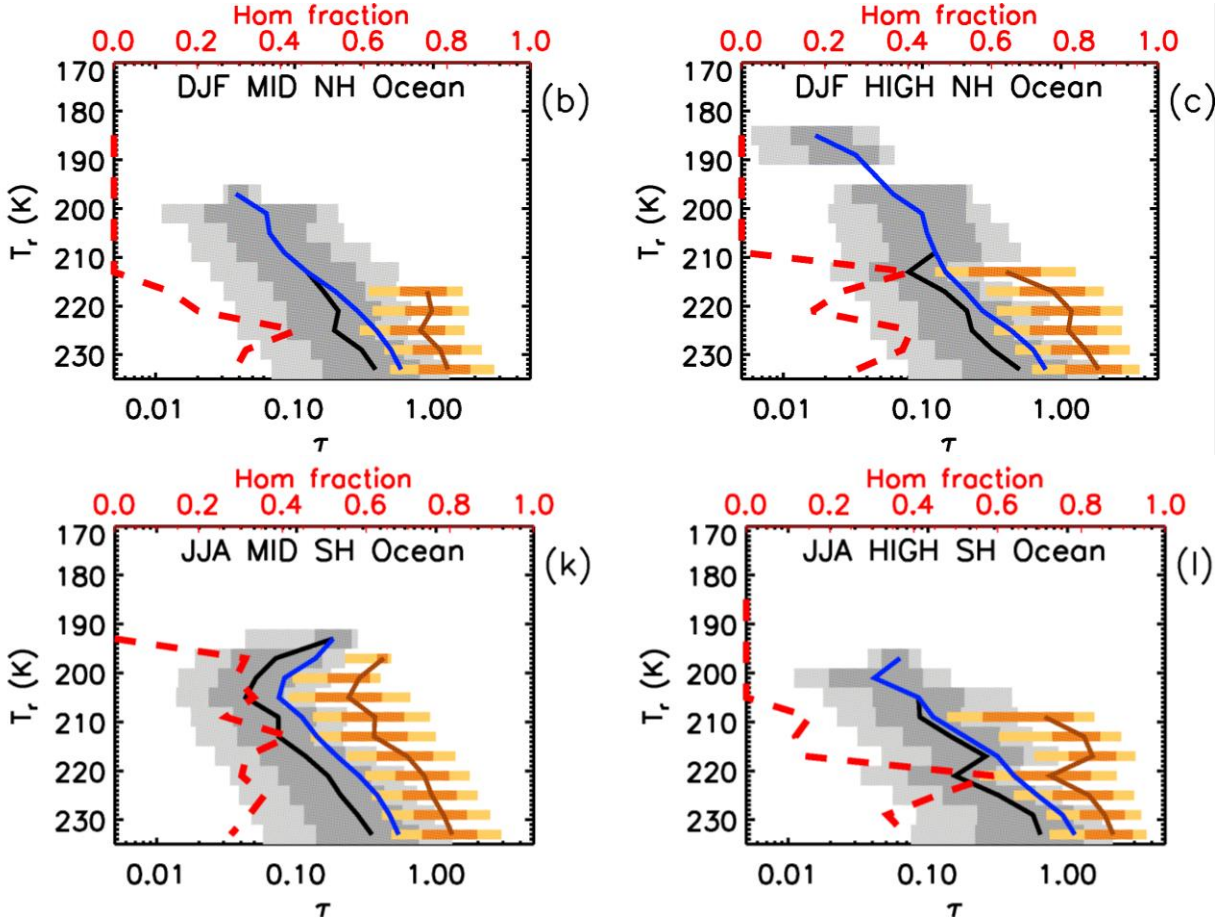

As in Fig. 18, but instead of showing median N_i profiles, median τ profiles are shown for all cirrus (blue), for het cirrus (black), and for hom cirrus (orange).

TREATMENT OF HOM IN ESMs: PRE-EXISTING ICE

Much of the discrepancy in GCM simulations of CCT may be due to the use or non-use of the treatment of pre-existing ice (Gasparini et al., 2020, ERL; Tully et al., 2023, ACP).

The pre-existing ice treatment described in Shi et al. (2015, ACP) is based on the supersaturation development equation that can be written as:

$$\frac{dS_i}{dt} = a_1 S_i W - (a_2 + a_3 S_i)\left(\frac{dq_{i,nuc}}{dt} + \frac{dq_{i,pre}}{dt}\right)$$

where $q_{i,nuc}$ is the ice mass mixing ratio due to nucleation and $q_{i,pre}$ is the ice mass mixing ratio of pre-existing ice, parameters a_1, a_2, and a_3 depend only on the ambient temperature and pressure, S_i is the supersaturation with respect to ice, W is the updraft velocity and t is time. From this equation it is seen that the greater $q_{i,pre}$ is, the smaller the increase in S_i is. As stated in Shi et al. (2015), “The pre-existing ice crystals significantly reduce ice number concentrations in cirrus clouds, especially at mid- to high latitudes in the upper troposphere (by a factor of ~ 10). Furthermore, the contribution of heterogeneous ice nucleation to cirrus ice crystal number increases considerably.”

From Shi et al. (2015, ACP): Contrast between CAM5 simulations not using the treatment of pre-existing ice (left) and using it (right). Note that the color legend values differ by a factor of 10. $N_i > 200\ L^{-1}$ can be attributed to homogeneous ice nucleation (i.e., hom).

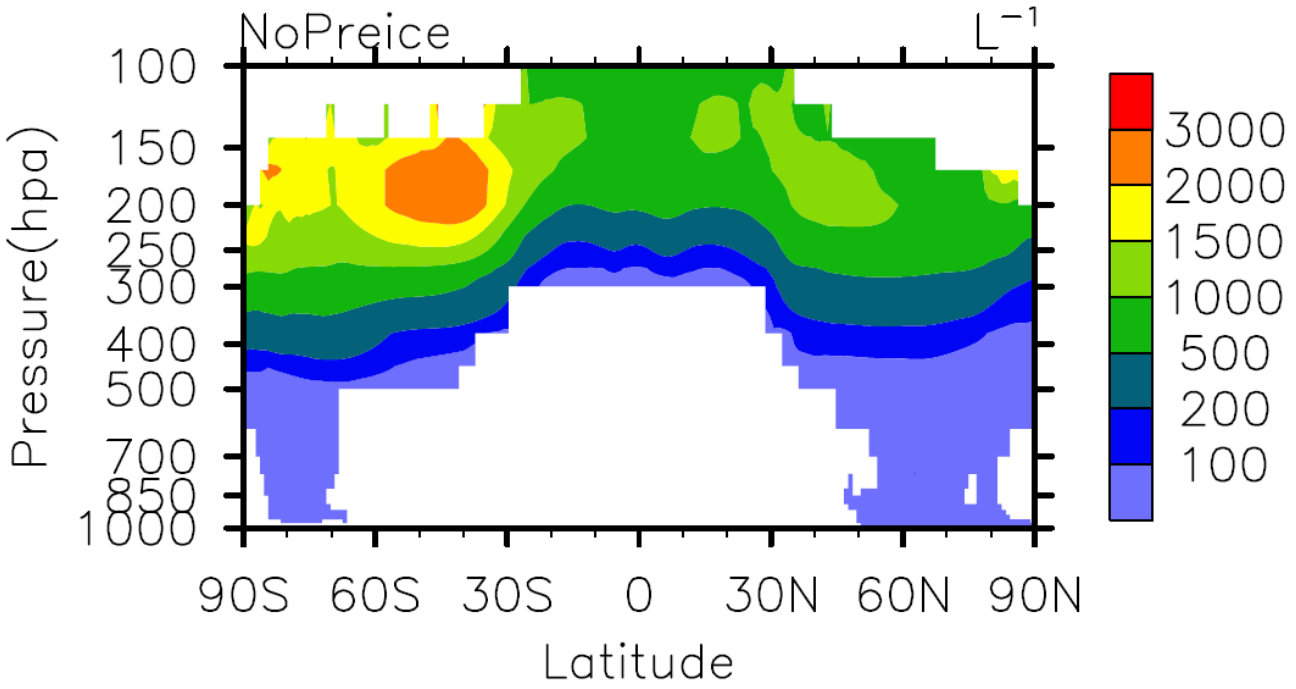

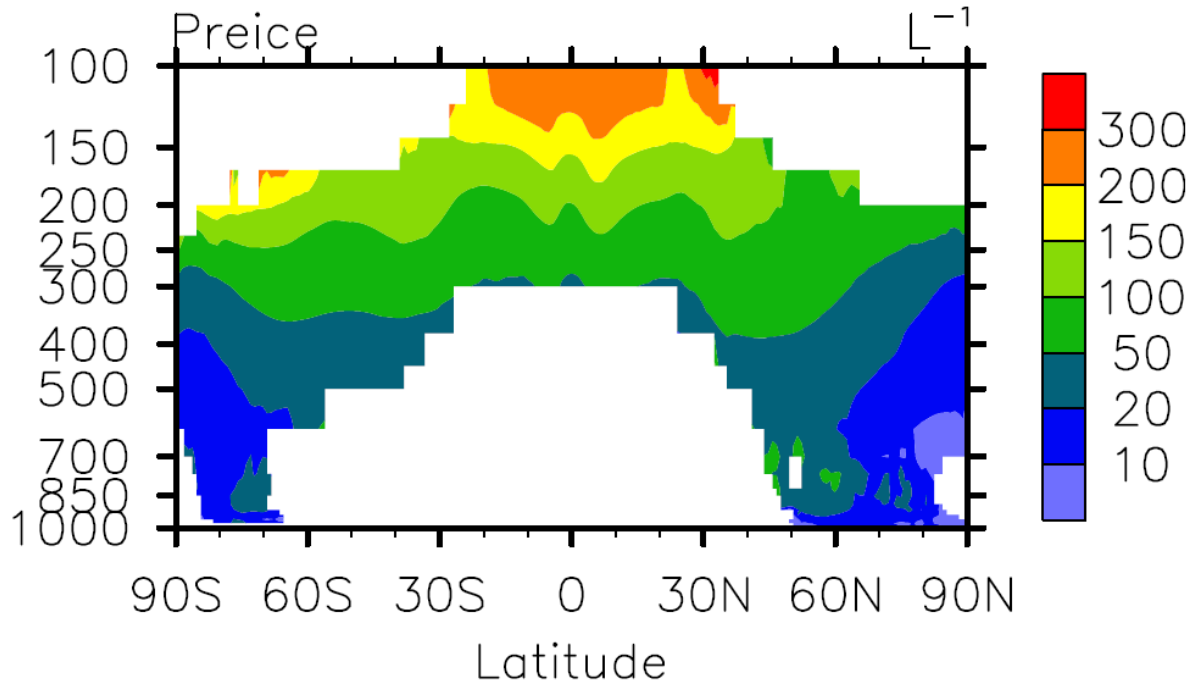

In-cloud RHi results from a remote sensing study by Dekoutsidis et al. (2023, ACP) for in situ and liquid origin cirrus clouds during the ML Cirrus field campaign. Note that RHi associated with homogeneous ice nucleation (i.e., hom), shown in blue, prevails near cloud top. This is consistent with Diao et al. (2015) with ice nucleation more active near cloud top, and it suggests relatively high concentrations of relatively small ice crystals near cloud top.

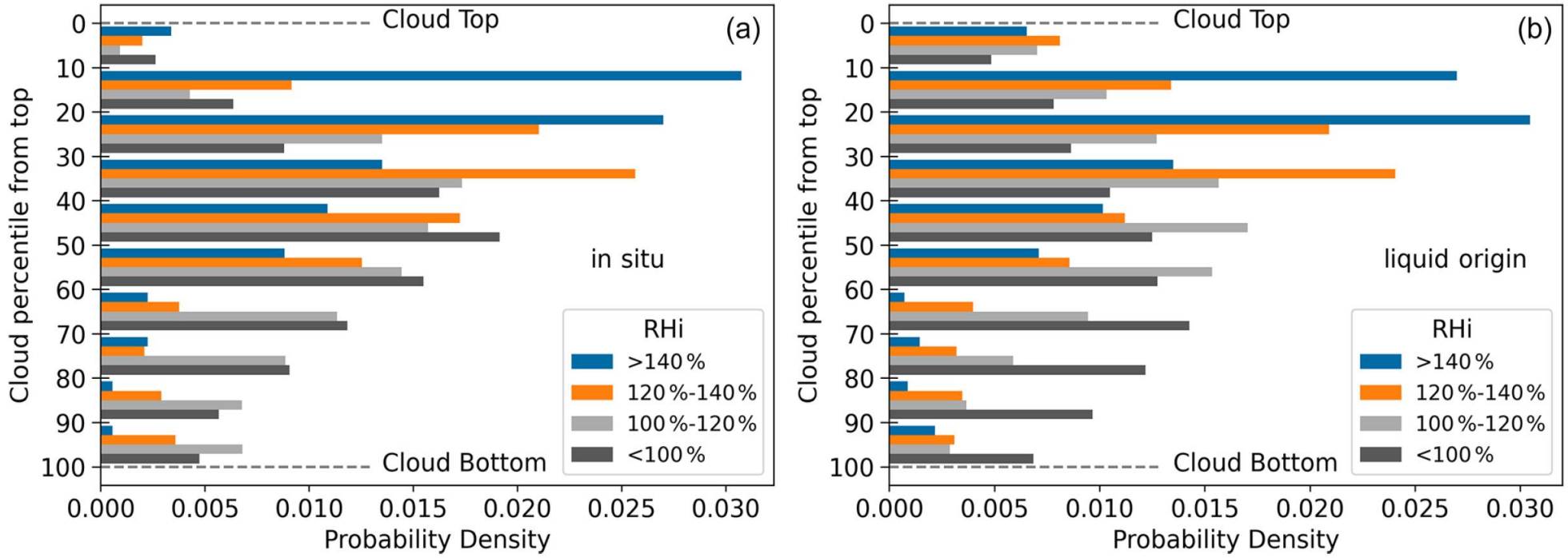

Figure 5. Probability densities of RHi in a relative location to the cloud top. **(a)** In situ clouds. **(b)** Liquid-origin clouds. For an in-detail description see Fig. 3.

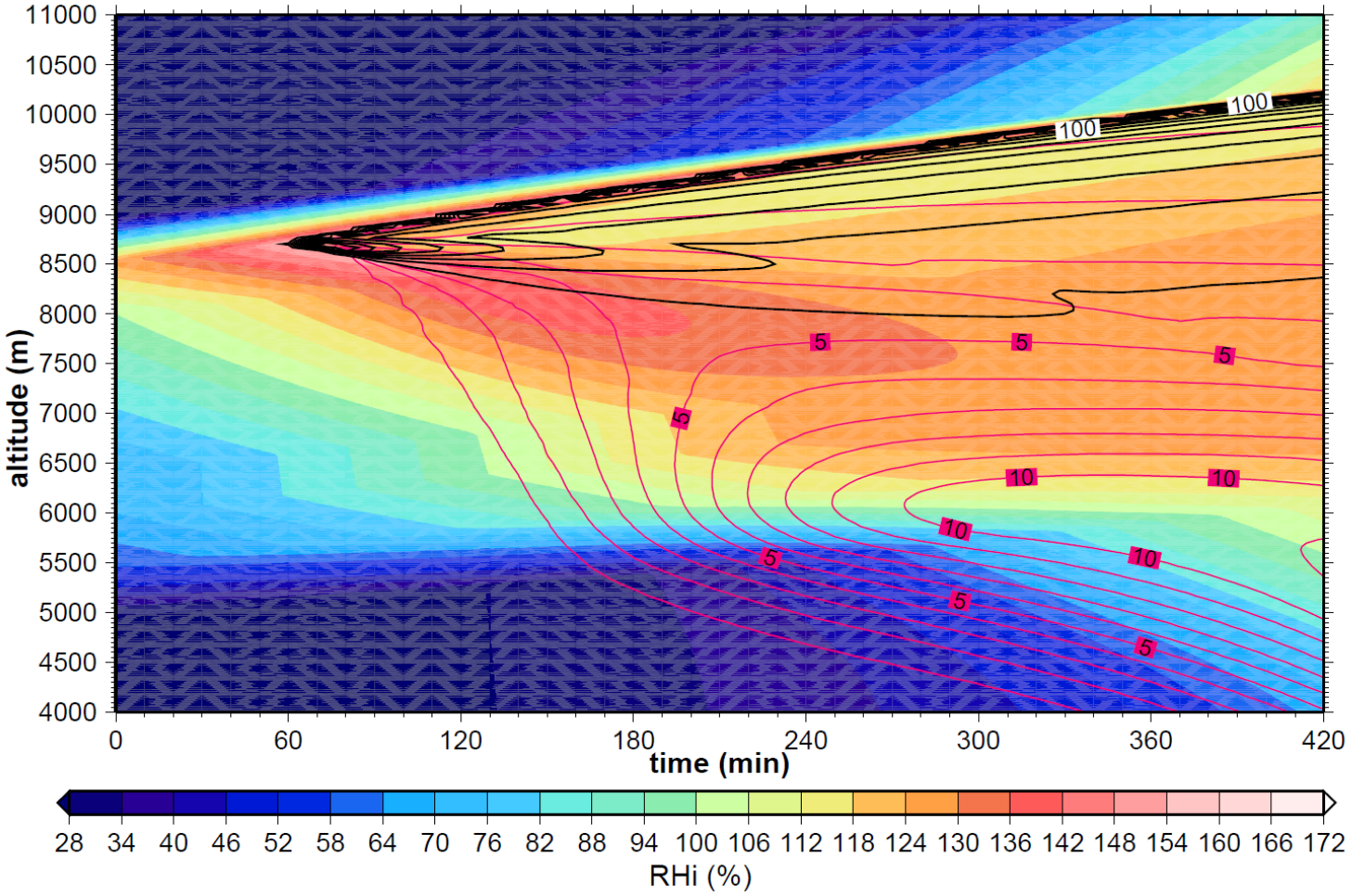

Fig. 15. Time evolution of the simulated cirrostratus lifted with a constant vertical velocity of w=0.05 m s^{-1}. The colours indicate relative humidity wrt ice, while lines indicate ice crystal number densities (black, in L^{-1}, Δn_c=10L^{-1}) and ice water content (purple, in mg m^{-3}, ΔIWC = 1mg m^{-3}).

From Spichtinger and Gierens, 2009, ACP: Modeling of cirrus clouds – Part 1a: Model description and validation.

Highest RHi and N_i is at cloud top where hom is active. To accurately predict N_i the continuous nucleation source at cloud top must be resolved, requiring 10 m vertical resolution. The cirrus cloud becomes thicker over time, with highest RHi and N_i when cloud is thinnest (consistent with CALIPSO results in Mitchell et al., 2018, ACP). IWC near cloud top ≈ 1/10th maximum IWC .

Reasons for questioning the pre-existing ice treatment:

1. Although it is theoretically robust, its implementation in GCMs is likely unrealistic due to a vertical resolution of ~ 700 m for cirrus clouds (in ECHAM-HAM).
   A. Observations and modeling show ice nucleation often proceeds through hom near cloud top where q_i is relatively low due to small ice crystal sizes and sedimentation.
   B. In a GCM cirrus layer, **it is likely that mean q_i >> actual q_i near cloud top**, thus overestimating the impact of pre-existing ice.

2. A new CALIPSO retrieval for cirrus cloud properties (N_i, D_e, IWC) has been used to estimate the fraction of cirrus clouds strongly affected by hom. Outside the tropics (± 30° latitude), the zonal mean hom fraction generally ranges from 20% to 35%. This is likely much higher than predicted in simulated cirrus from GCMs using the standard treatment of pre-existing ice.

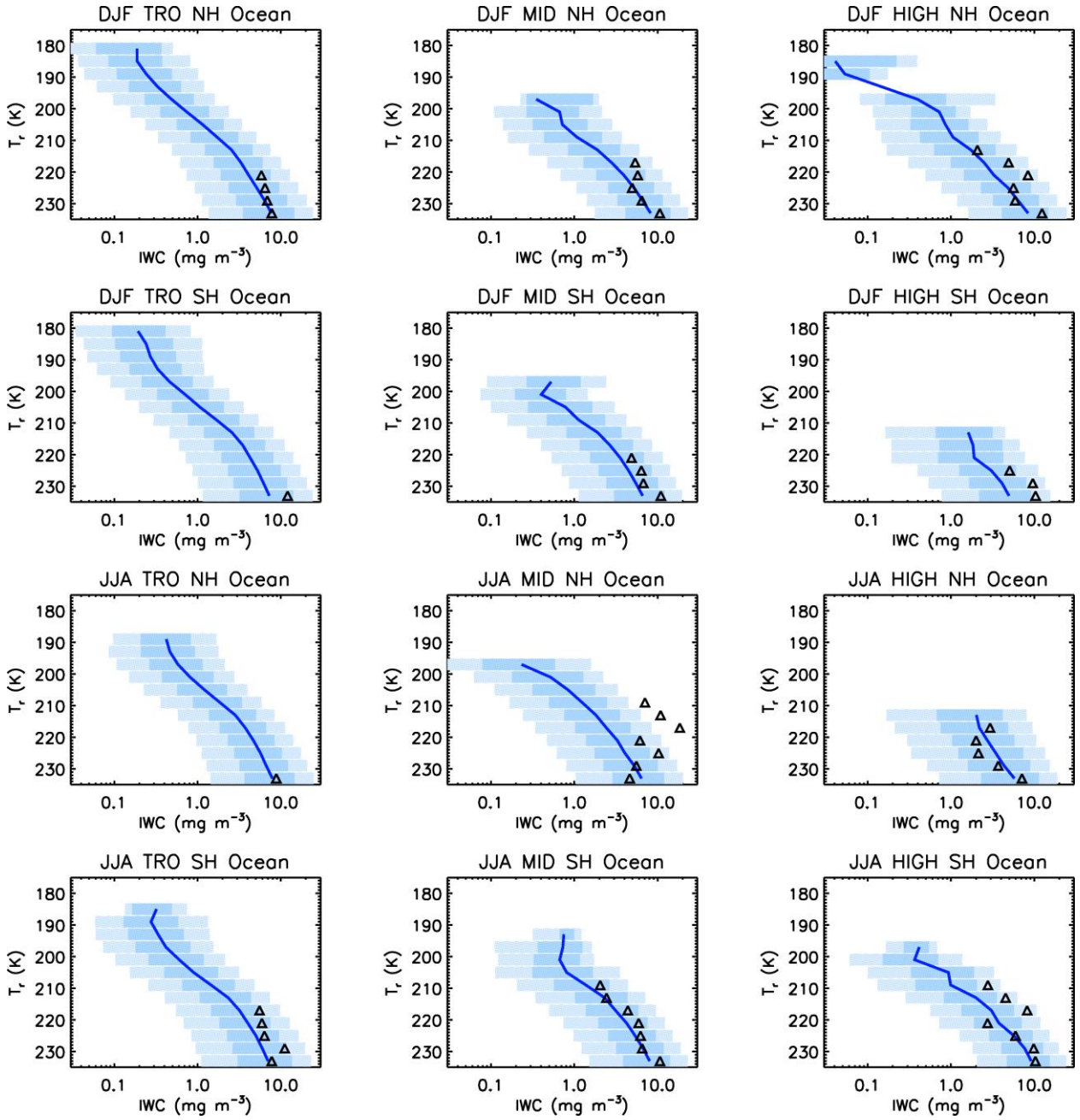

Comparing the median IWC (navy blue curves) over oceans (using all samples) with the temperature-dependent het-hom transition point (black triangles) based on the D_e maximum and the corresponding extinction coefficient α_{ext} for a given 4 K temperature interval. Latitude zones and seasons (winter and summer) are denoted as before. Medium-blue shade lies between the 25th and 75th percentiles while light-blue shade lies between the 10th and 25th and the 75th and 90th percentiles.

To a first approximation, the median IWC divides the het and hom regimes.

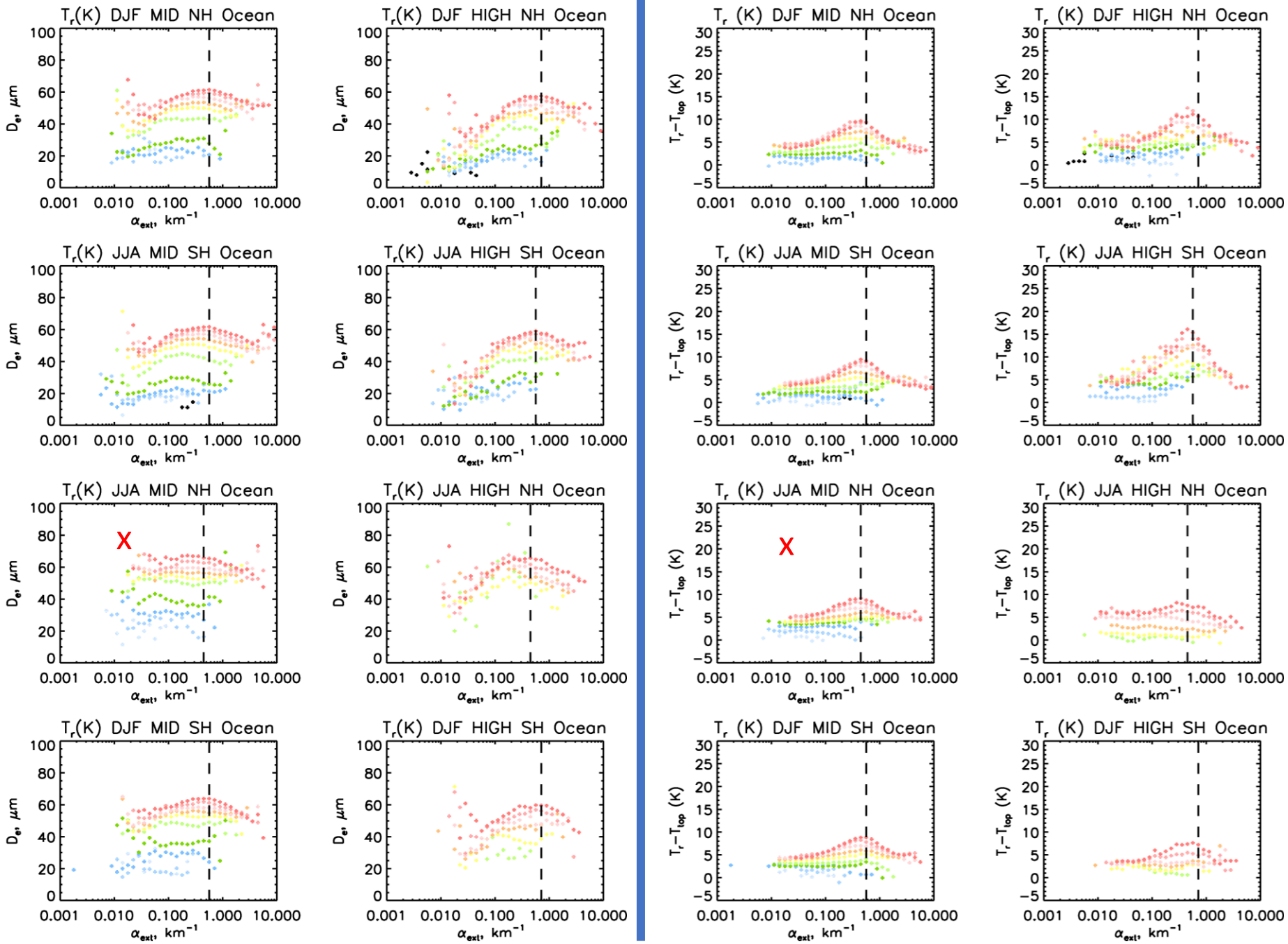

Right side: T_r = cloud radiative temperature, T_{top} = cloud top temp., $T_r - T_{top}$ is a measure of cloud geometrical depth. Left side shows D_e vs. $\log(\alpha_{ext})$ and the right side shows $T_r - T_{top}$ vs. $\log(\alpha_{ext})$ for various lat. zones and seasons. For all cases except one (indicated by X), **the maxima in D_e and $T_r - T_{top}$ at the highest temperatures occur at the same α_{ext}**. We postulate that this is not a coincidence but rather this is an important observation that reveals some of the physics of cirrus cloud formation.

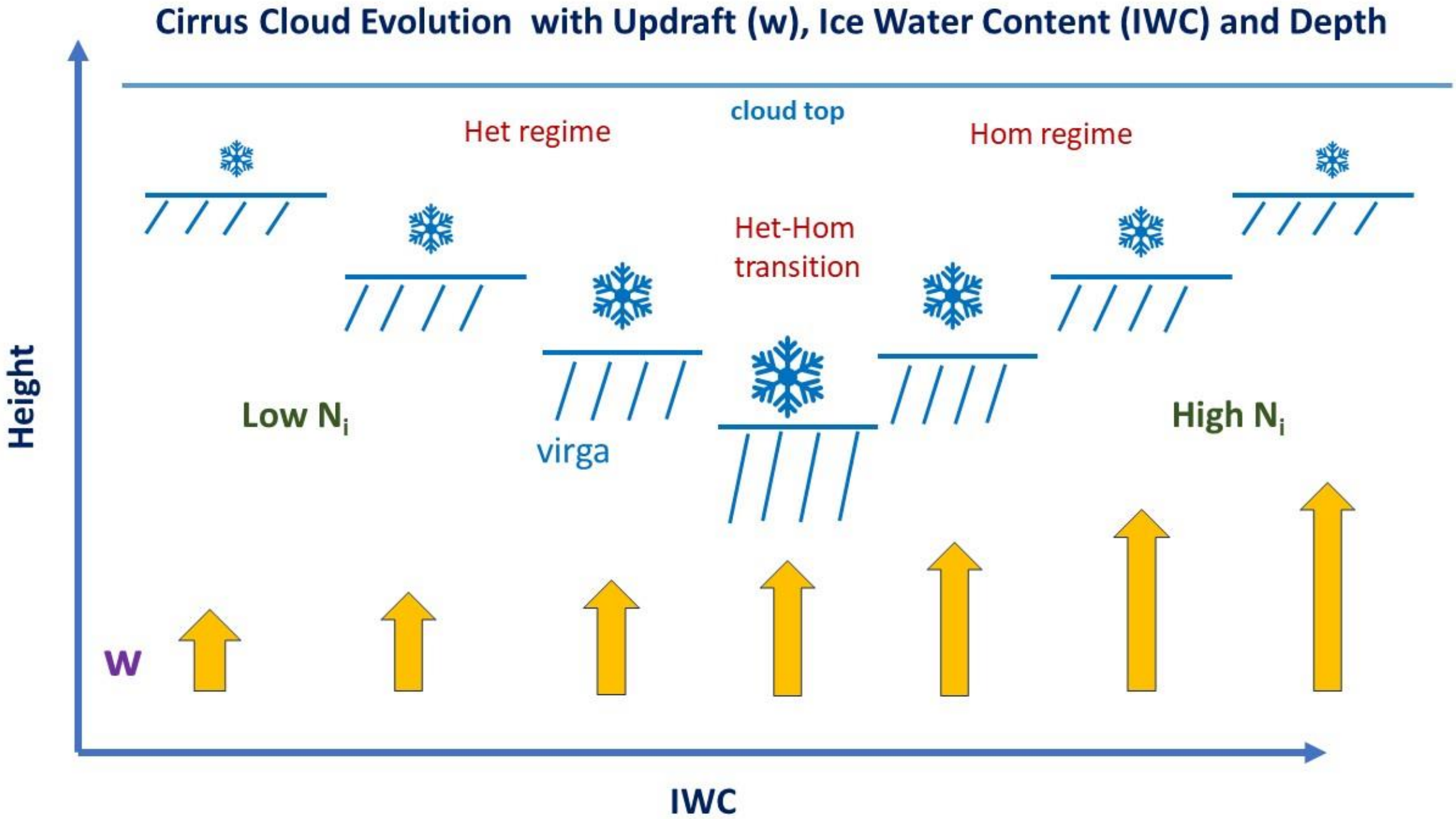
Cirrus Cloud Evolution with Updraft (w), Ice Water Content (IWC) and Depth
cloud top
Het regime
Hom regime
Het-Hom transition
Low N_i
virga
High N_i
w
Height
IWC

All samples over oceans; ~ 0.005 < OD < ~ 3. Color inside the triangles (from model) uses the same color code.